Electronic Supplementary Material (ESI) for Dalton Transactions.
This journal is © The Royal Society of Chemistry 2015

Dual-Targeting Organometallic Ruthenium(II) Anticancer Complexes Bearing EGFR-Inhibiting 4-Anilinoquinazoline Ligands

Yang Zhang, Wei Zheng,* Qun Luo, Yao Zhao, Erlong Zhang, Suyan Liu, and Fuyi Wang*

Supporting Information

1. **Synthesis of 4-anilinoquinazoline derivatives L2 – L14**
2. **Figure S1 – S19**

Synthesis of 4-anilinoquinazoline derivatives L2 – L14

General procedure of the preparation of compounds L2 – L5: To a suspension of compound L1 (4.0 g, 17 mmol) in 80 mL sulfoxide chloride, 1.5 mL DMF was added and the resulting mixture was heated to reflux for 4 h. Then solvent was removed in vacuum and the residues was solidified after cooling to ambient temperature, washed with diethyl ether successively to give the product (L2) as light yellow powder (3.0 g, yield 69.8%). After that, 6.0 mmol L2, 6.0 mmol substituted aniline (3'-chloro-4'-fluoroaniline, 3-aminobenzonitrile or 3-aminoanisole) were mixed in 80 mL isopropanol and the resulting mixture was heated to reflux and stirred for 3 h. After cooling to ambient temperature, the solid was collected by filtrating, recrystallised from ethanol to give compounds L3 (1.74g, yield 80.1%), L4 (1.5g, yield 75.3%), and L5 (1.72g, yield 85.0%).

General procedure of the preparation of compounds L6 – L8**:** The as-prepared compound L3, L4 or L5 (4.5 mmol) were suspended in 100 mL absolute methanol, and sodium methoxide (10 mmol) was added and stirred at ambient temperature for 0.5 h. The solvent was removed in vacuum and 100 mL water was added to the residue and pH was regulated to 2.0, the appeared solid was collected by filtration and washed by water, recrystallised from ethanol to give compounds L6 (1.26g, yield 88%), L7 (1.20g, yield 90%), and L8 (1.12g, yield 85%).

General procedure of the preparation of compounds L9 – L12**:** The as-prepared compound L6, L7 or L8 (3.4 mmol) and potassium carbonate (18 mmol) were mixed in 16 mL DMF. Then 1,2-dibromoethane or 1,3-dibromopropane (14 mmol) was added and the resulting mixture was heated and stirred at 80 °C for 5 h. After cooling to ambient temperature and filtering in vacuum, the filtrate was collected and poured into 70 mL water, followed by extraction using ethyl acetate (20 mL × 4), organic layers were combined and dried over magnesium sulfate. After concentration, the residue was chromatographed by flash chromatography on Silica gel using ethyl

acetate/petroleum (5:1) as eluent to give compounds L9 (0.94g, yield 65.0%), L10 (0.10g, yield 70%), L11 (0.9g, yield 66.7%), and L12 (0.7g, yield 50.0%).

General procedure of the preparation of compounds L13 – L14**:** The as-prepared compound L9, L10 (1.2 mmol) was dissolved in 20 mL acetonitrile and ethylenediamine (12 mmol) was added. The resulting mixture was heated to reflux and stirred for 2.5 h. Then the solvent was evaporated in vacuum and the residue was recrystallised from water and ethanol to give L13 (4-(3'-chloro-4'-fluoroanilino)-6-(2-(2-aminoethyl)aminoethoxy)-7-methoxyquinazoli-ne, 0.34g, yield 72.1%), or chromatographed by flash chromatography on silica gel using methanol/dichloromethane/ammonia (5:1:0.05) as eluent to give L14 (4-(3'-chloro-4'-fluoroanilino)-6-(3-(2-aminoethyl)aminopropoxy)-7-methoxyquinazol-ine, 0.33g, yield 65.8%) as white powder.

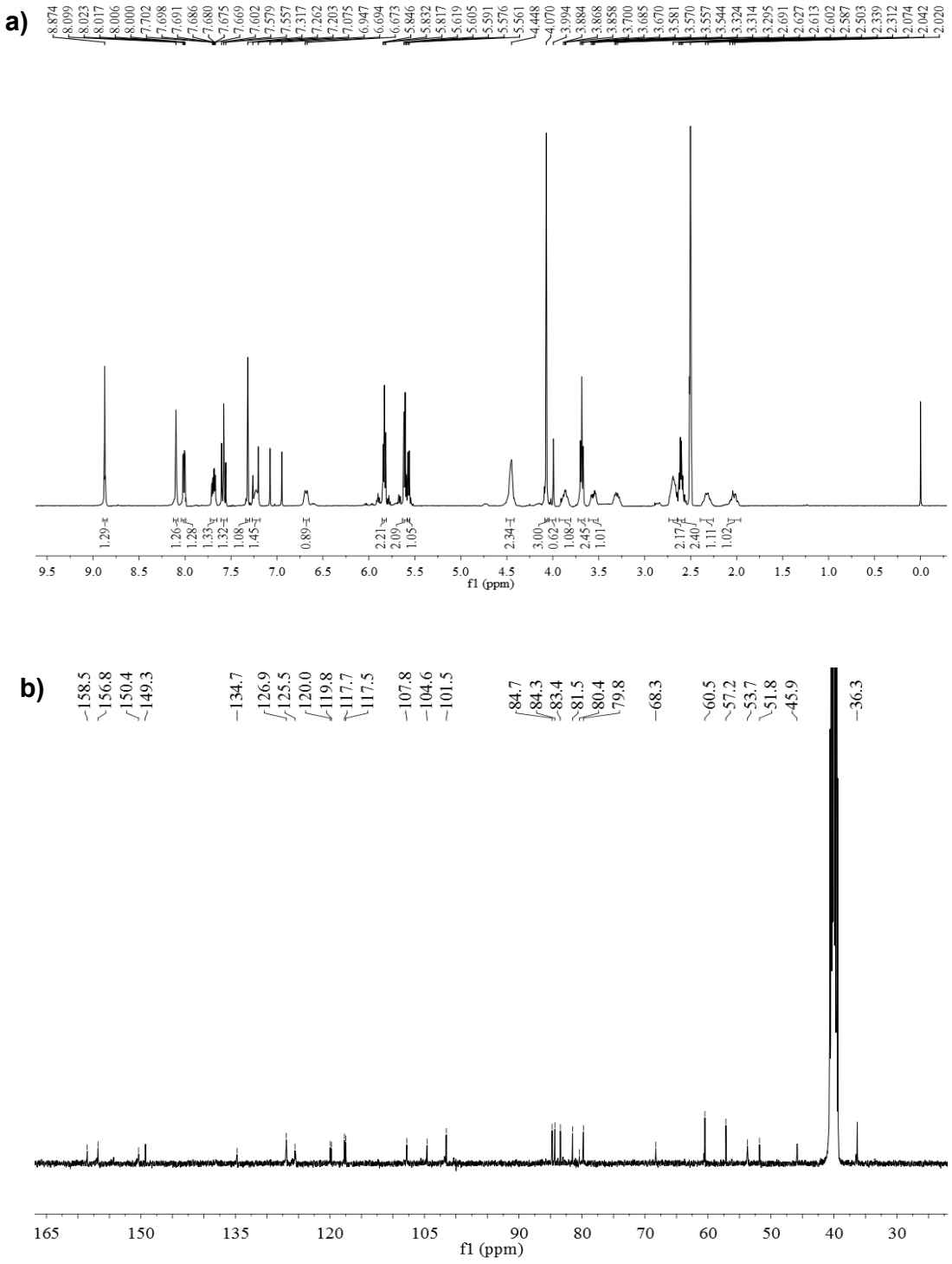

Figure S1. (a) ^{1}H NMR, (b) ^{13}C NMR spectra of complex **7**.

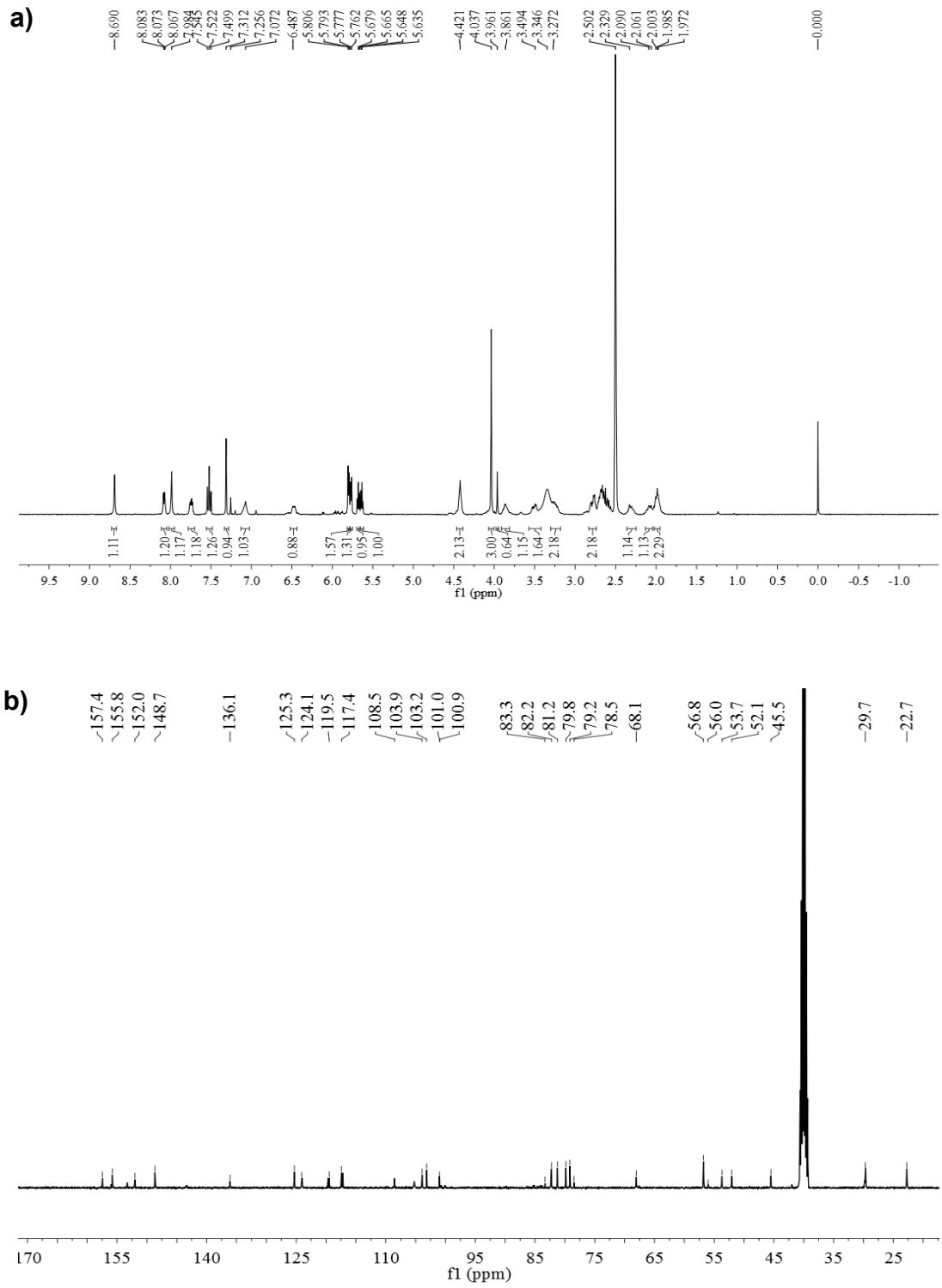

Figure S2. (a) ^{1}H NMR, (b) ^{13}C NMR spectra of complex **8**.

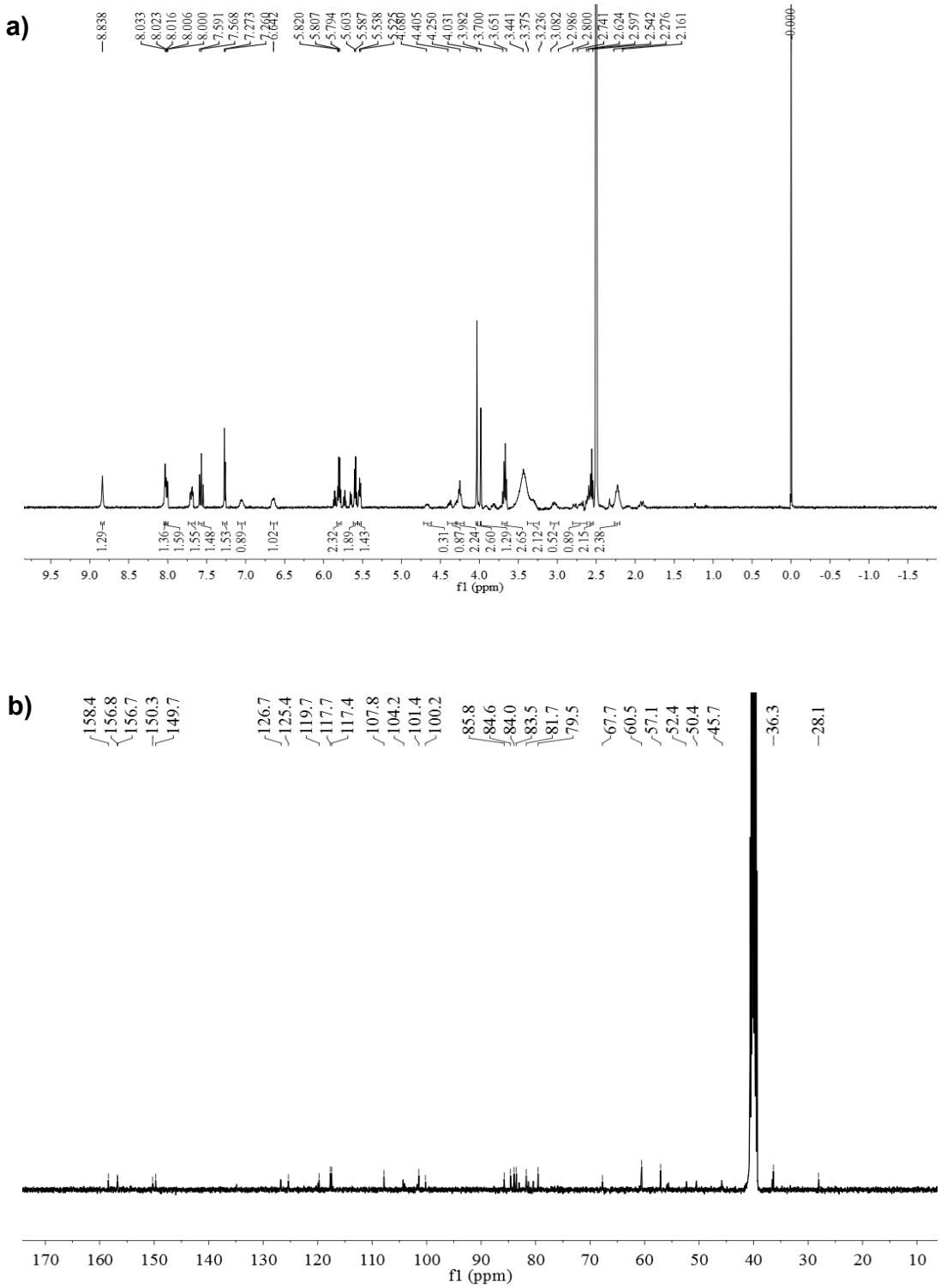

Figure 3. (a) ^{1}H NMR, (b) ^{13}C NMR spectra of complex **9**.

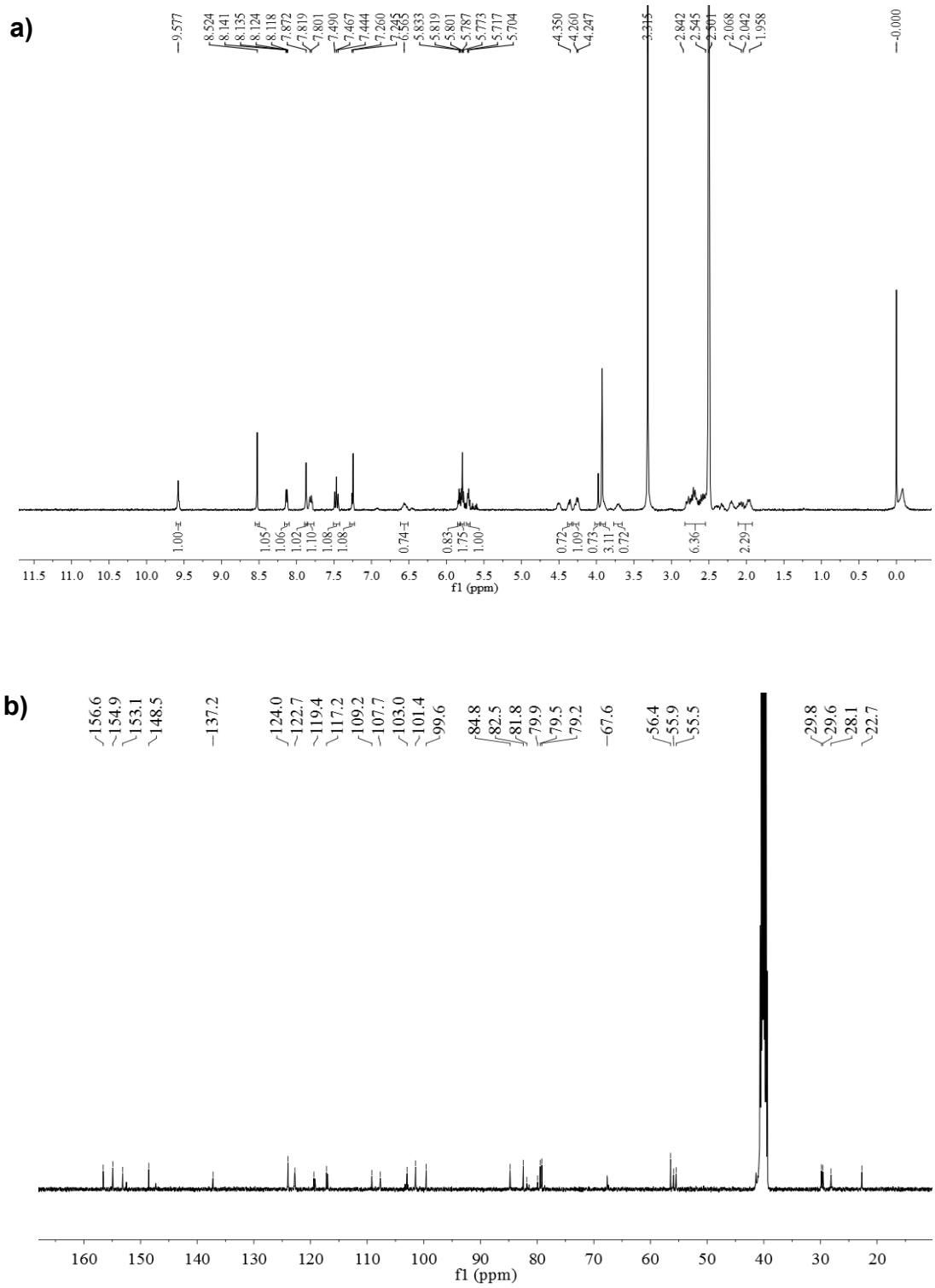

Figure S4. (a) ^{1}H NMR, (b) ^{13}C NMR spectra of complex **10**.

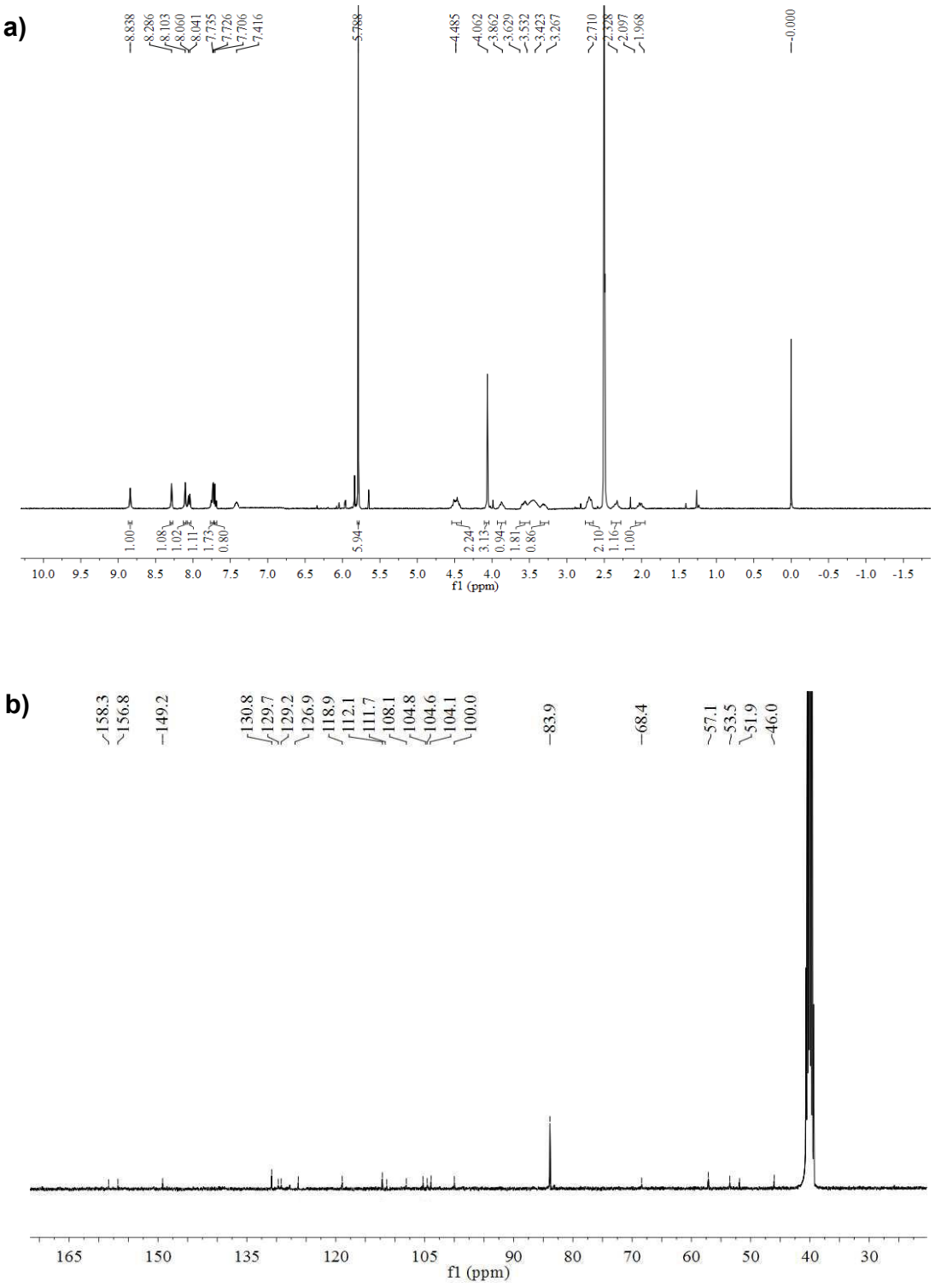

Figure S5. (a) ^{1}H NMR, (b) ^{13}C NMR spectra of complex **11**.

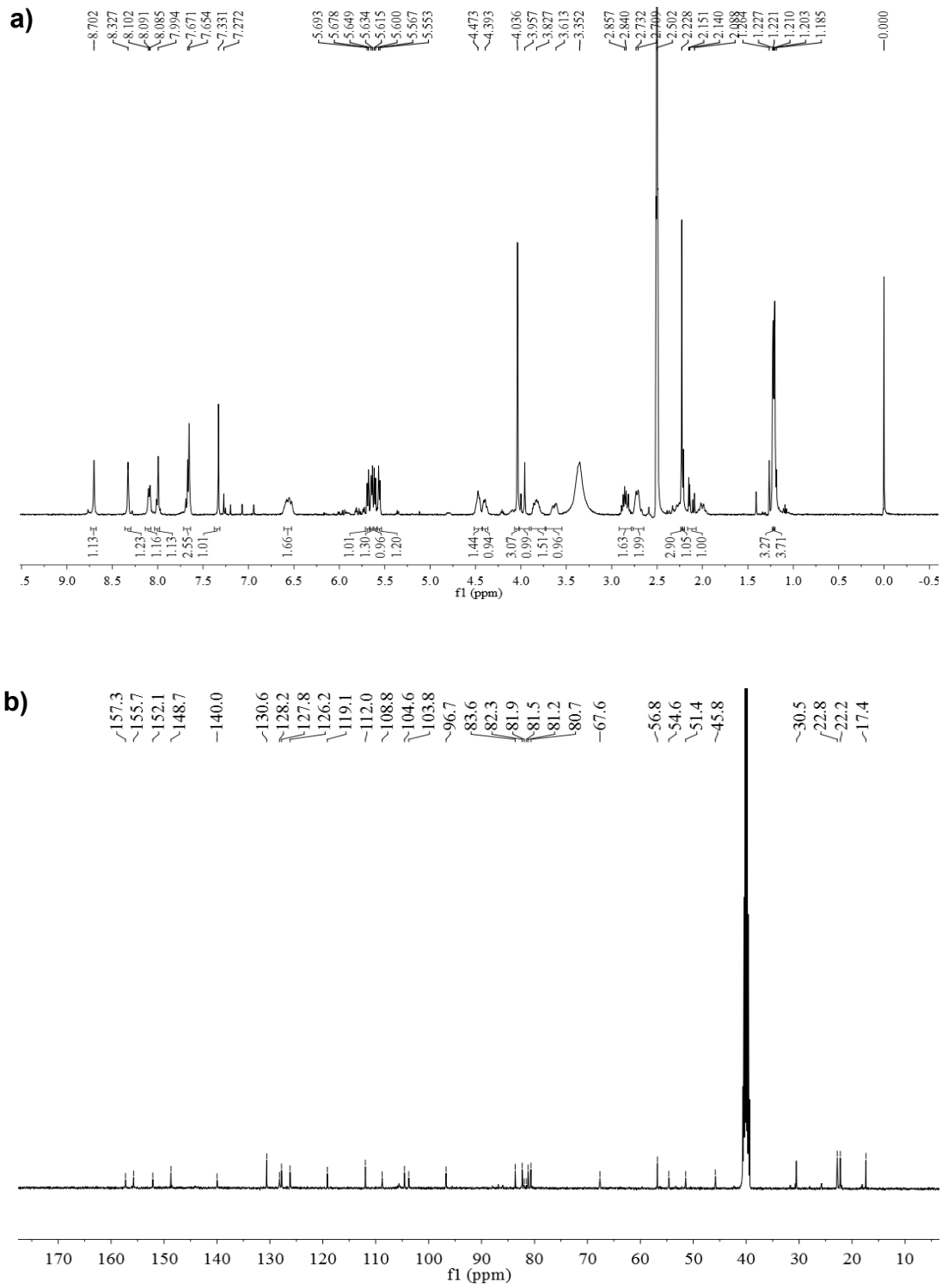

Figure S6. (a) ^{1}H NMR, (b) ^{13}C NMR spectra of complex **12**.

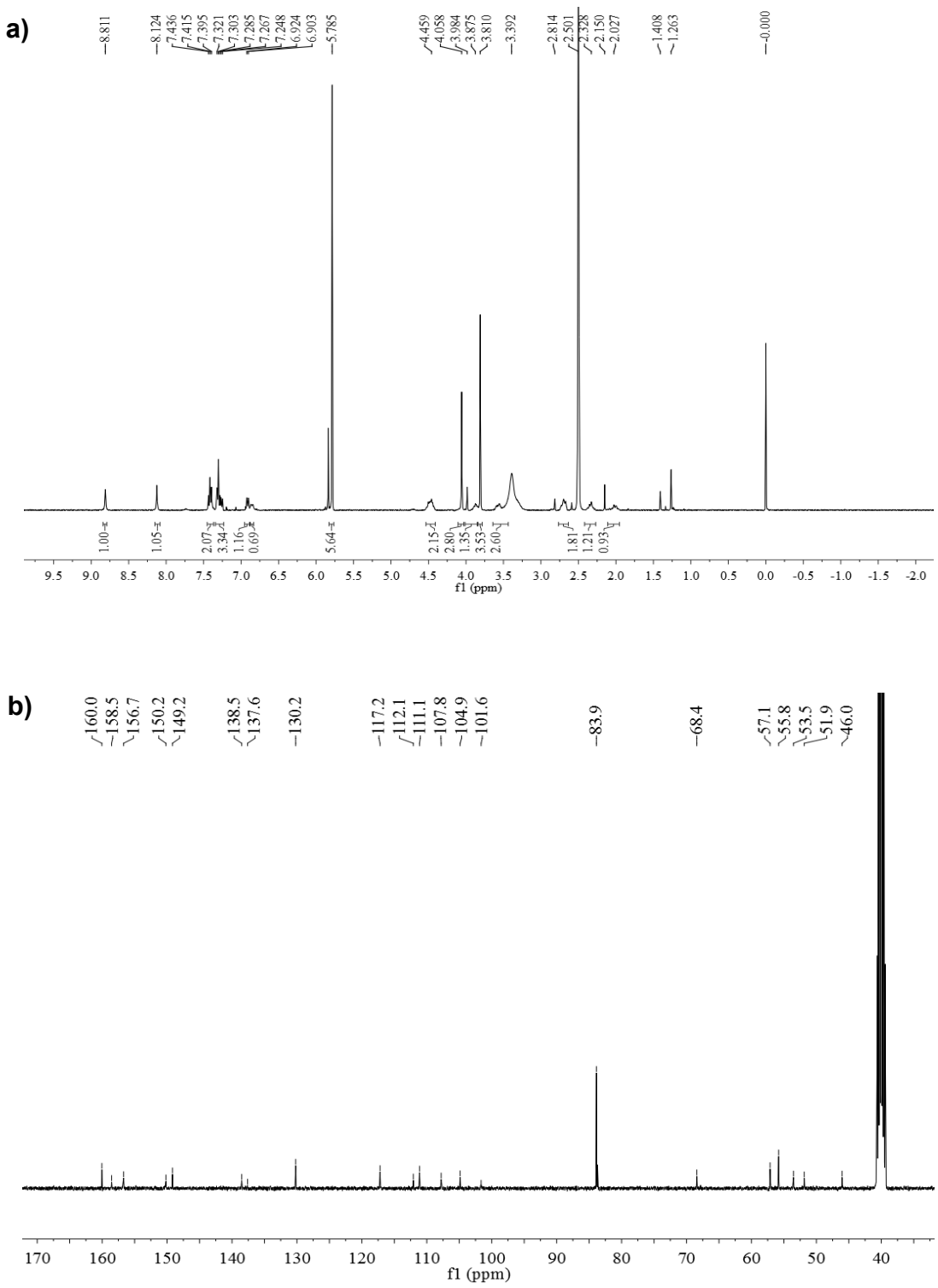

Figure S7. (a) ^{1}H NMR, (b) ^{13}C NMR spectra of complex **13**.

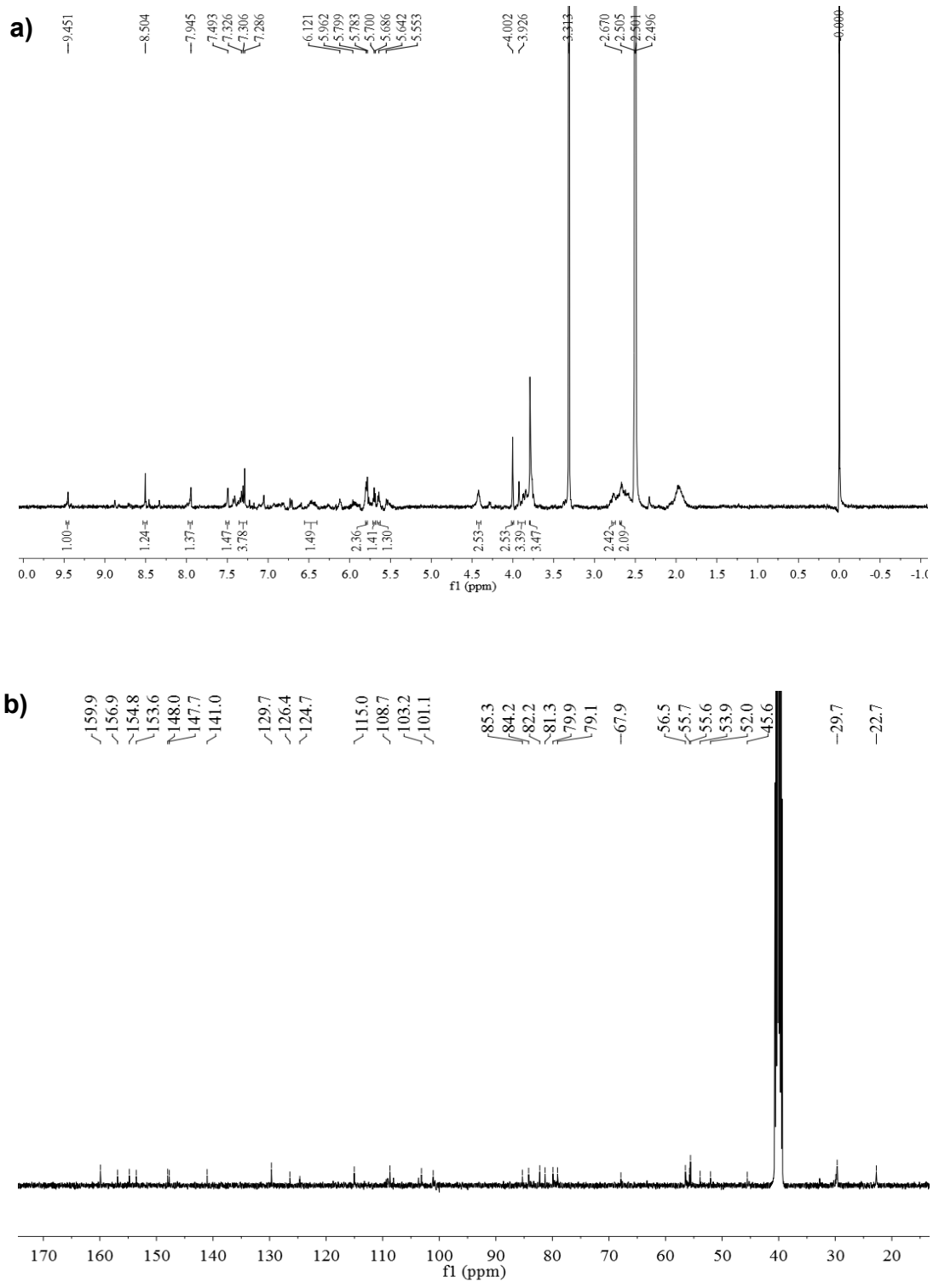

Figure S8. (a) ^{1}H NMR, (b) ^{13}C NMR spectra of complex **14**.

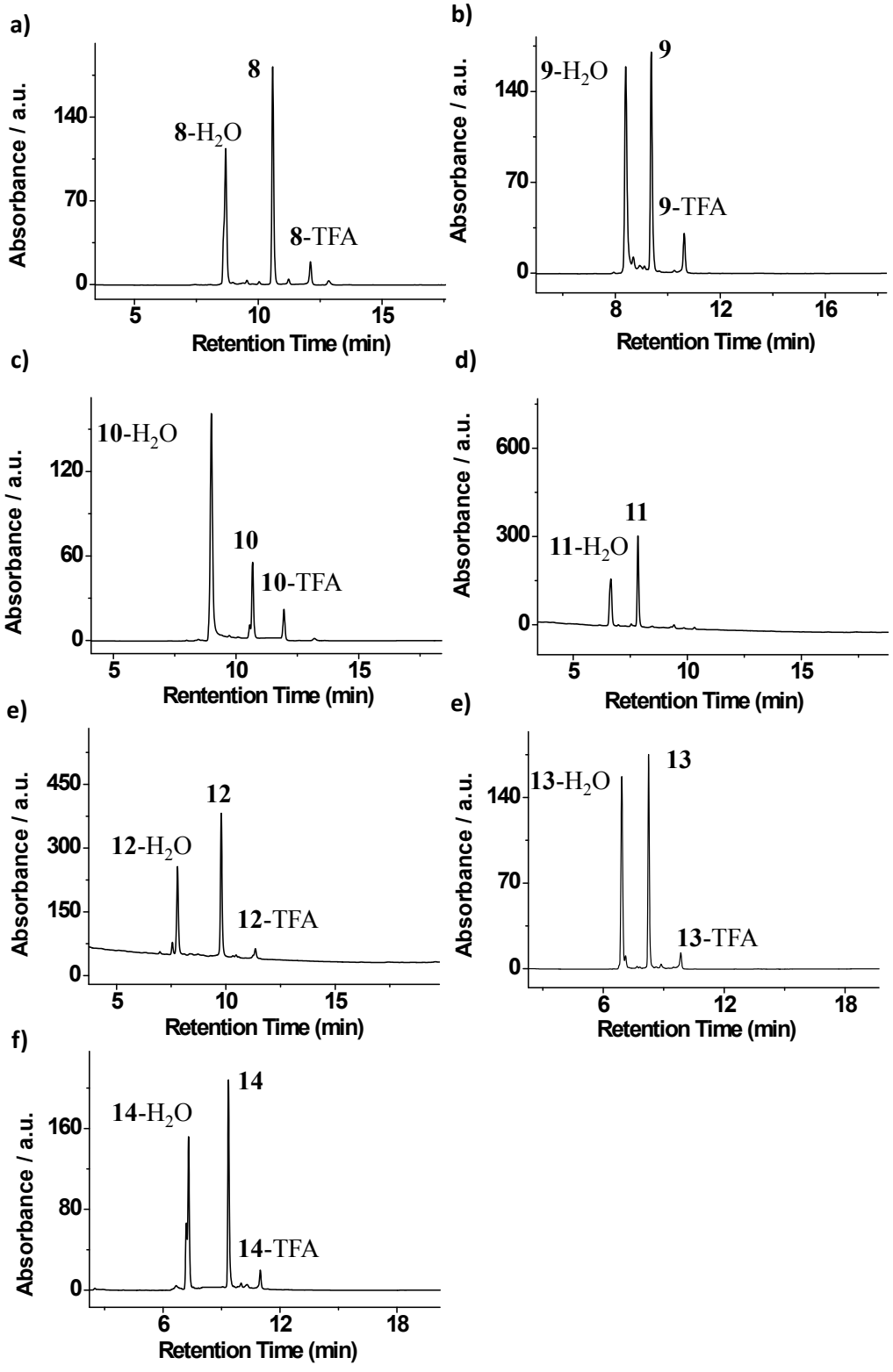

Figure S9. HPLC chromatograms with UV detection at 360 nm of complexes **8** – **14** (0.1 mM) in aqueous solution incubated at 298 K for 2 h.

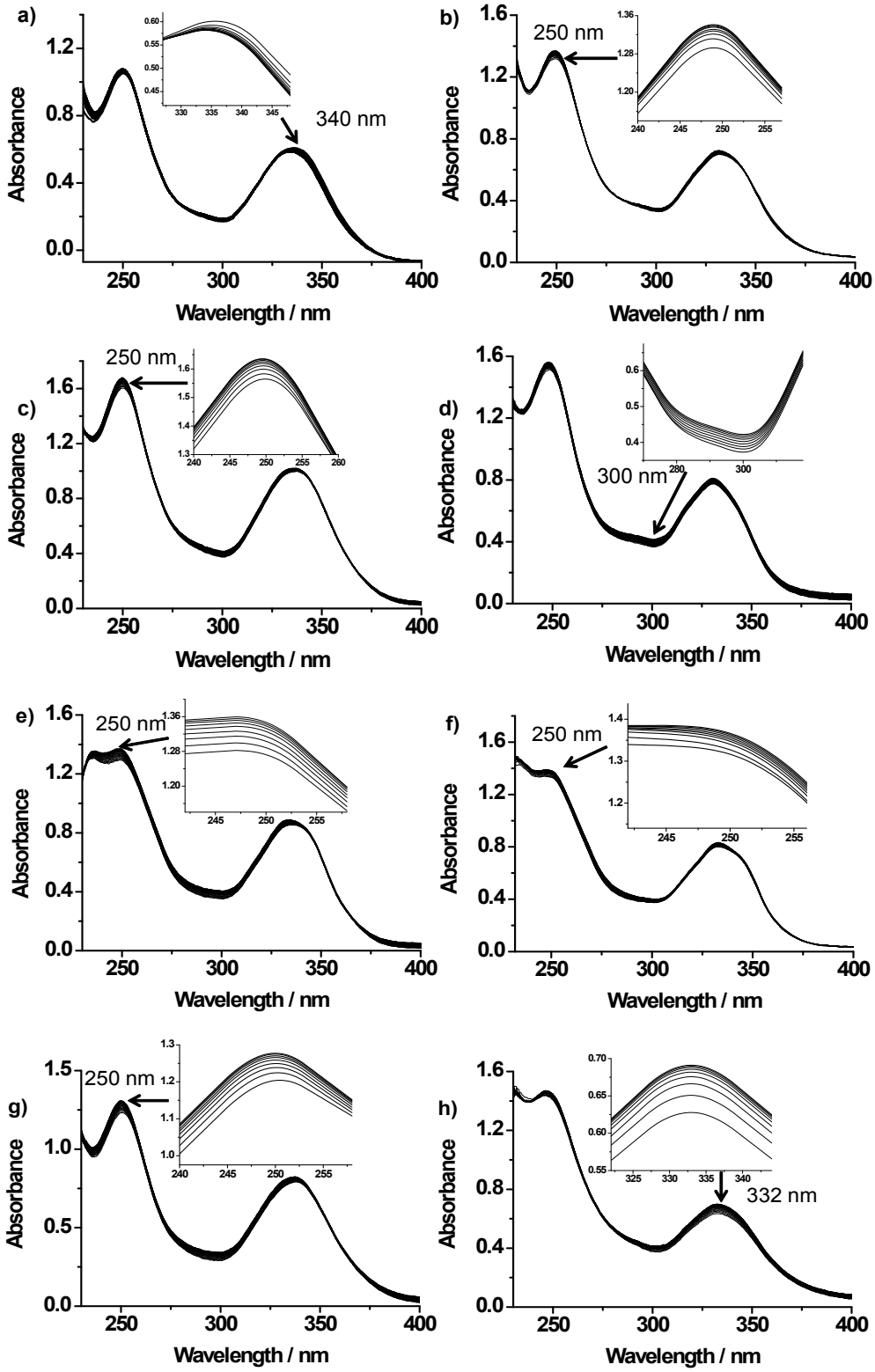

Figure S10. Time evolution of UV-Vis differential spectra for the aquation of 50 μM (a) **7**, (b) **8**, (c) **9**, (d) **10**, (e) **11**, (f) **12**, (g) **13**, (h) **14** in aqueous solution at 298 K from 0 – 120 min. The arrows indicate the wavelengths selected for kinetic studies.

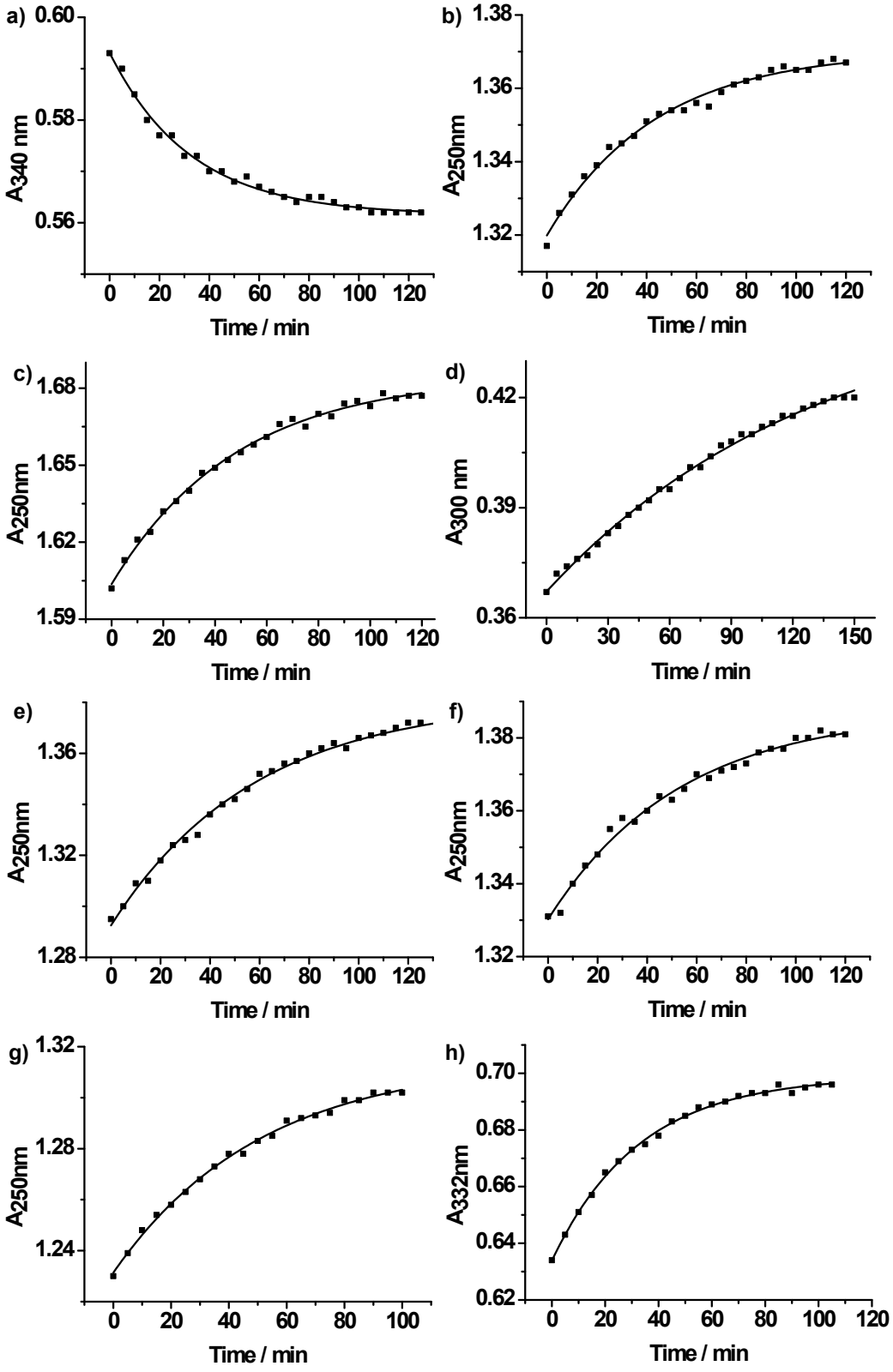

Figure S11. Time-dependence of the absorbance at selected wavelengths for the hydrolysis of 50 μM (a) **7**, (b) **8**, (c) **9**, (d) **10**, (e) **11**, (f) **12**, (g) **13**, (h) **14** in aqueous solution at 298 K.

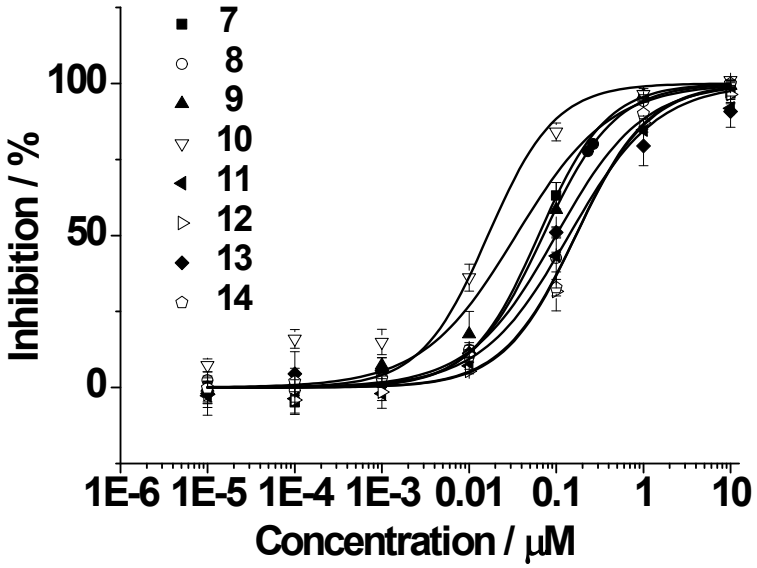

Figure S12. Concentration-response curves of inhibition efficiency of arene ruthenium(II) complexes **7 – 14** on EGFR. Points: mean ± SD of triplicate determinations. Lines: computer-fitting results.

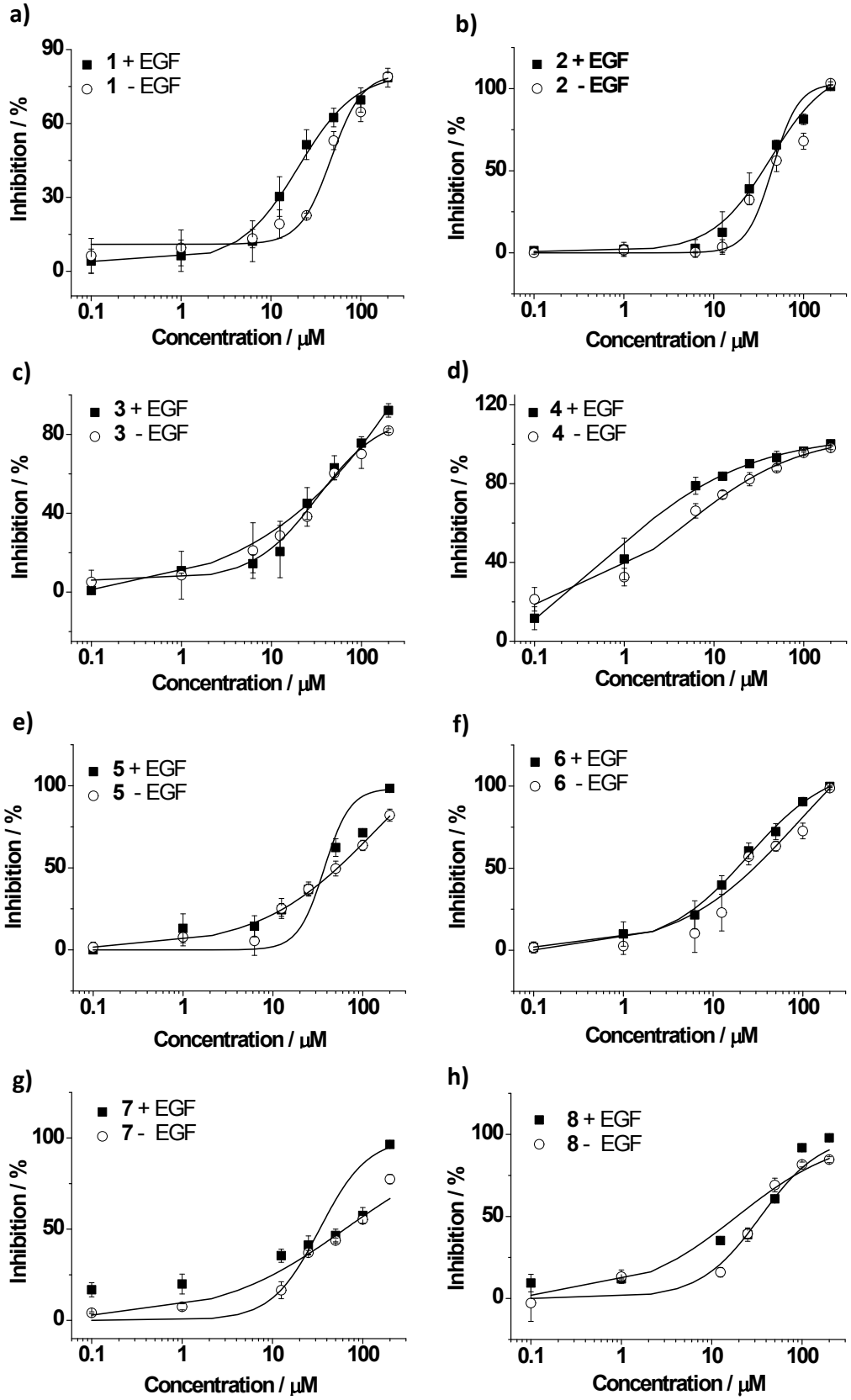

Figure S13. Dose-dependent inhibition curves of complexes (a) **1**; (b) **2**; (c) **3;** (d) **4**; (e) **5**; (f) **6**; (g) **7** and (h) **8** on the proliferation of HeLa cancer cell line in the absence or the presence of EGF (100 ng·mL^{-1}).

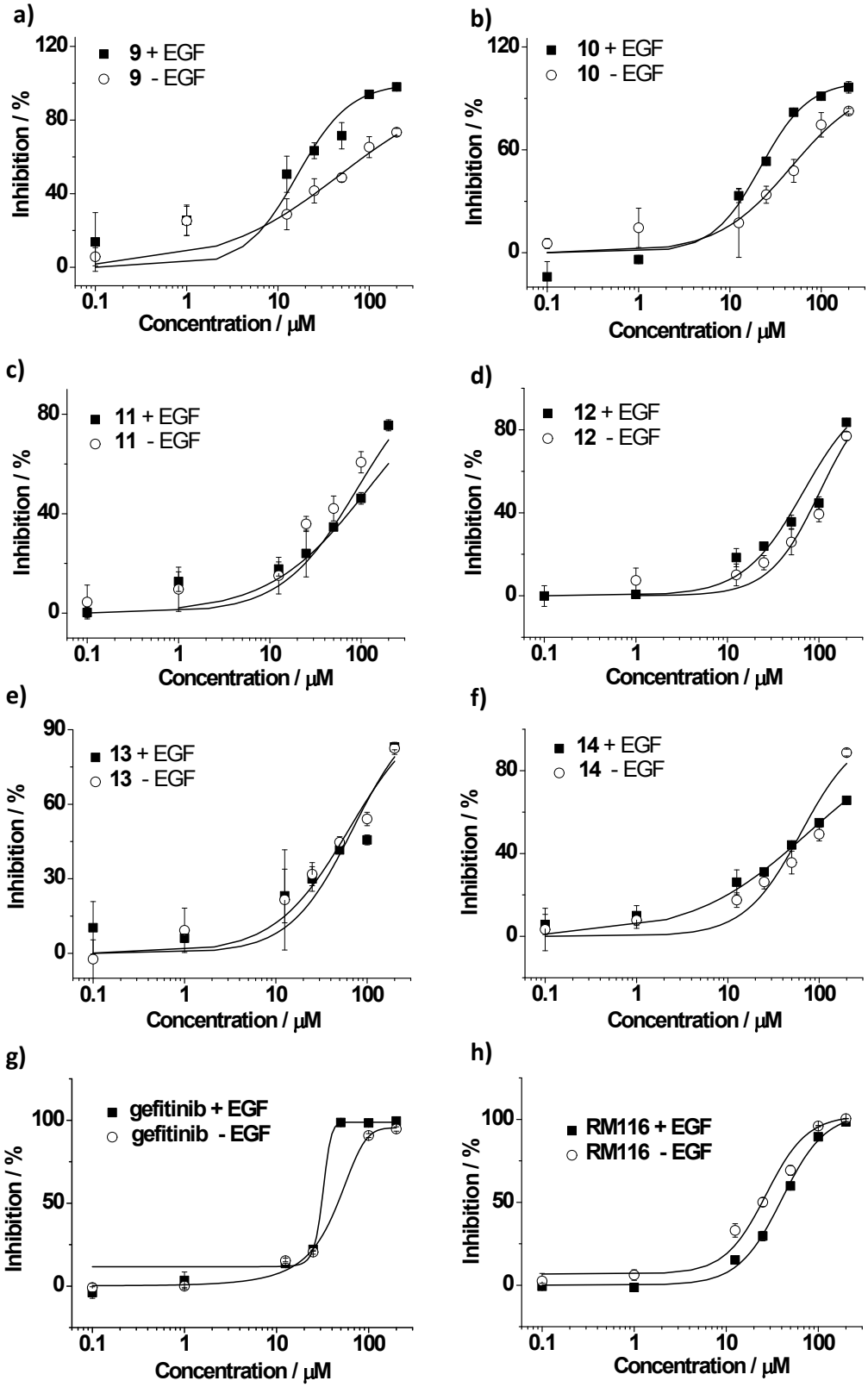

Figure S14. Dose-dependent inhibition curves of complexes (a) **9**; (b) **10**; (c) **11;** (d) **12**; (e) **13**; (f) **14**; (g) gefitinib and (h) RM116 on the proliferation of HeLa cancer cell line in the absence or the presence of EGF (100 $ng \cdot mL^{-1}$).

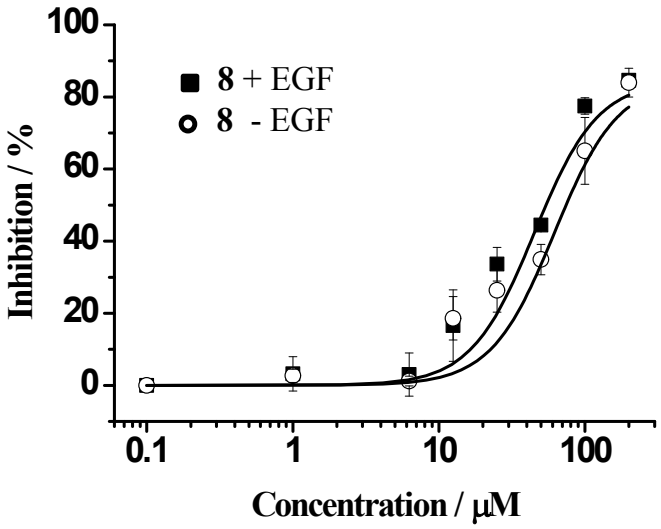

Figure S15. Dose-dependent inhibition curves of complex **8** on the proliferation of HEB normal cell line in the absence (-) or the presence (+) of EGF (100 ng·mL^{-1}).

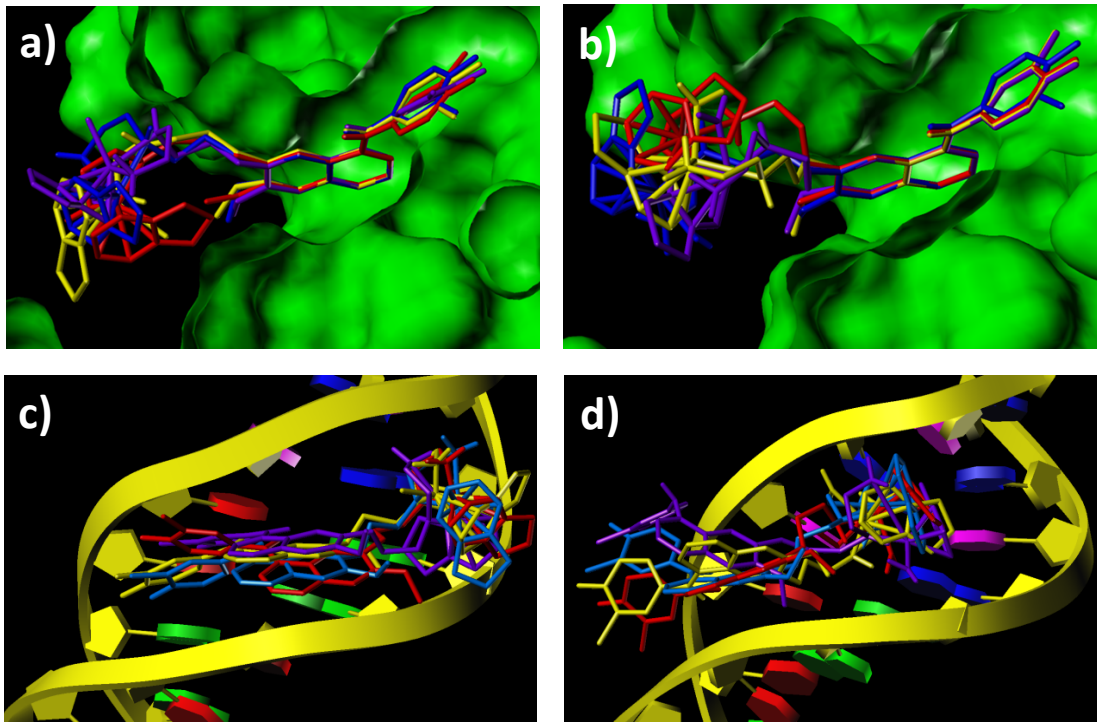

Figure S16. (a, b) The detailed conformation of the ATP-binding pocket housing the cations of chiral complex (a) **8** and (b) **8** in aqua form in four different configurations. (c, d) Docking poses of the cations of chiral complex (c) **8** and (d) **8** in aqua form in four different configurations into the minor groove of the DNA duplex 5′-d(CGCGAATTCGCG)·d(CGCGAATTCGCG)-3′ (**I**). **8**-(*RR*) and **8**-(*RR*)-aqua in red, **8**-(*RS*) and **8**-(*RS*)-aqua are shown in blue, **8**-(*SR*) and **8**-(*SR*)-aqua in yellow, and **8**-(S*S*) and **8**-(S*S*)-aqua in purple. EGFR are shown in green surface; DNA is shown in ribbon with G in blue, C in pink, A in green and T in red. Docking scores of **8**-(*RR*), **8**-(*RS*), **8**-(*SR*), and **8**-(*SS*) were 6.94, 6.88, 6.91, and 6.82 into EGFR; and 5.27, 5.13, 5.32, and 5.25 into DNA, respectively. Docking scores of **8**-(*RR*)-*aqua*, **8**-(*RS*)-*aqua*, **8**-(*SR*)-*aqua*, and **8**-(*SS*)-*aqua* were 9.07, 8.91, 8.86, and 9.00 into EGFR; 6.71, 6.60, 6.78, and 6.63 to DNA, respectively.

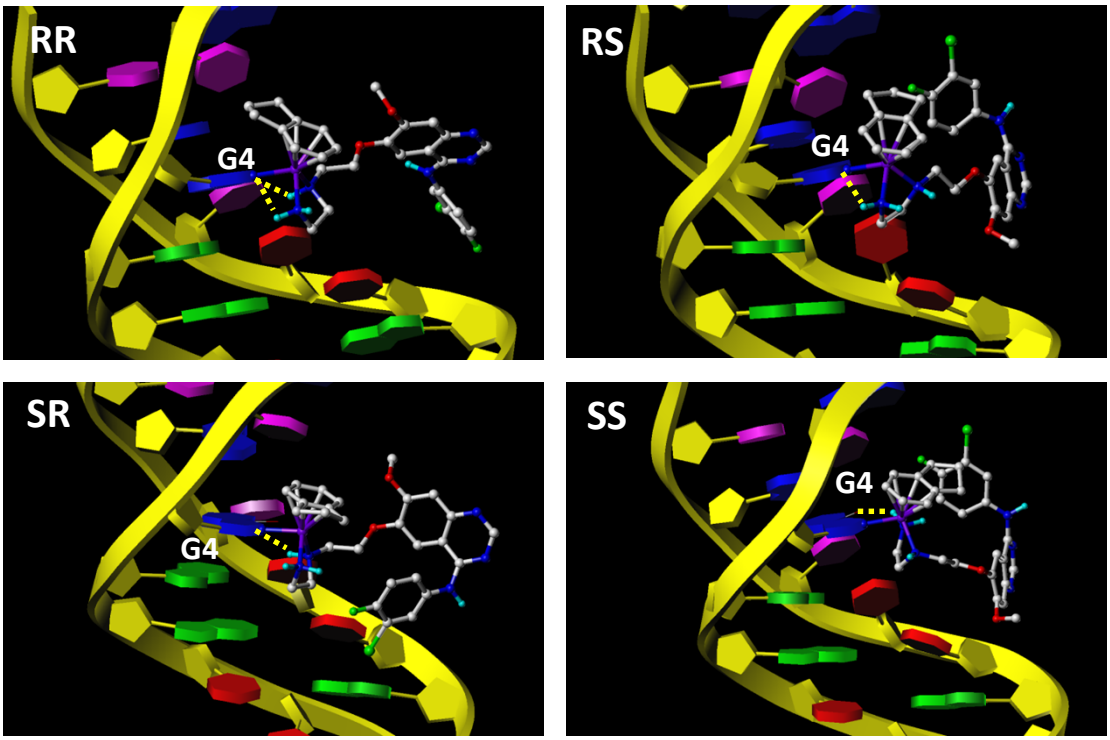

Figure S17. The detailed conformation of the cations of four stereoisomers of complex **8** binding to N7 of G4 in DNA duplex **I**. DNA is shown in ribbon with G in blue, C in pink, A in green and T in red. Binding energy of **8**-(*RR*), **8**-(*RS*), **8**-(*SR*), and **8**-(*SS*) to G4-N7 were −119, −120, −121, and −117 kcal•mol^{-1}, respectively.

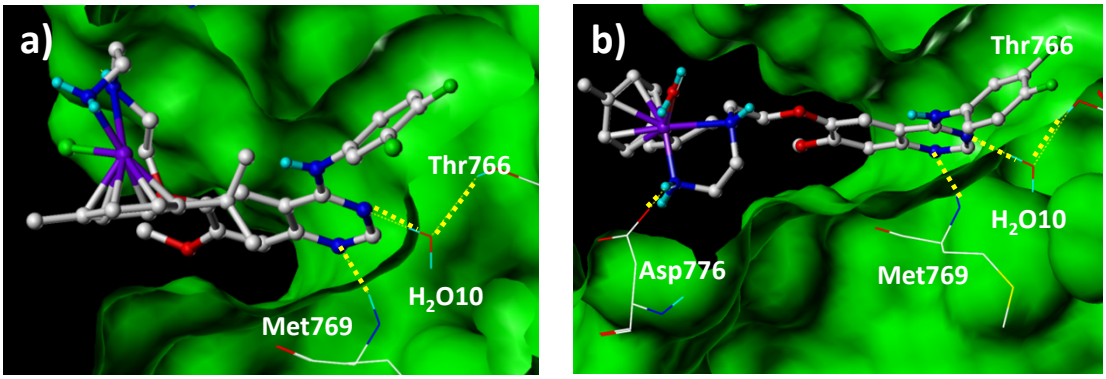

Figure S18. The detailed conformation of the ATP-binding pocket housing the cations of complexes (a) **2** and (b) **2** in aqua form. The residues of EGFR are shown in sticks with O atoms in red, N atoms in blue, S atoms in yellow and C atoms in grey. The dotted yellow lines illustrate the positions of H-bonding interactions.

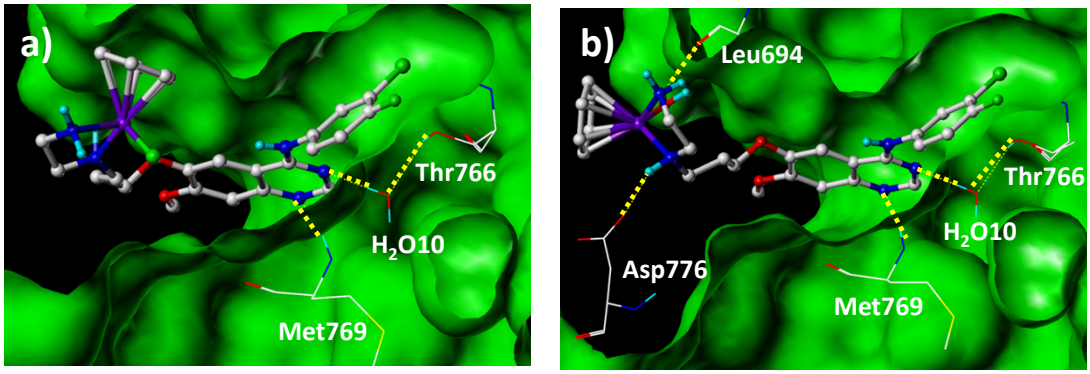

Figure S19. The detailed conformation of the ATP-binding pocket housing the cations of complexes (a) **4** and (b) **4** in aqua form. The residues of EGFR are shown in sticks with O atoms in red, N atoms in blue, S atoms in yellow and C atoms in grey. The dotted yellow lines illustrate the positions of H-bonding interactions.